Study of the ^{4}He Crystal Surface

K.O. Keshishev, V.I. Marchenko, and D.B. Shemyatikhin

Kapitza Institute for Physical Problems, RAS, Moscow, 119334 Russia

The evolution of the meniscus of a helium crystal near the (0001) face is traced during a change in the boundary conditions at the chamber wall in the temperature range 0.5-0.9 K. The critical behavior of the contact angle is studied. An anisotropy is detected in the crystal-glass interface energy. New data on the temperature dependence of the elementary-step energy are obtained.

In this work, we continue to study the behavior of the contact angle that appears when the interface of two condensed phases of ^{4}He (crystal-superfluid) reaches a solid wall. The formulation of the problem and a detailed description of our optical technique were given in our earlier works [1, 2]. Recall only that the technique consists in photographing a crystal using parallel light followed by digital processing of images. To improve the images, we substantially modified the cryostat design. In the modified version, an optical tract passes through windows located in the vacuum space of the cryostat and does not meet liquid helium. As a result, we were able to decrease the image noise by several times.

Figure 1 schematically shows the cross section of the experimental chamber with a crystal at the bottom. Recall also that, when analyzing the meniscus profile near the chamber walls, we consider a two-dimensional problem in the section plane, since the longitudinal chamber size (29 mm) is significantly larger than the capillary constant $\lambda \sim 1$ mm. The crystal is oriented so that the (0001) basal plane is horizontal. The x, z plane of a Cartesian coordinate system coincides with the section plane and axis z is vertical. Due to the chosen configuration of the side walls, the interface has an S-like shape described by a $Z(x)$ function. Then, angle

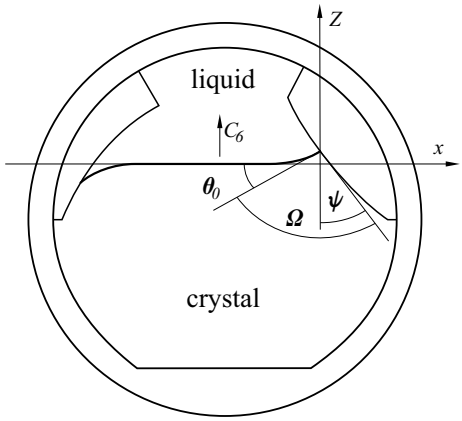

Fig. 1. Cross section of the experimental chamber

$\theta = arctg(dZ/dx)$ determines the surface inclination at a given point with respect to the (0001) plane. At the point of the end of surface at the wall, we have $\theta = \theta_0$, and θ_0 is one of the quantities to be measured in our experiment. The second quantity to be measured is the angle of wall inclination ψ to axis C_6 of the crystal at the contact point.

Angle of contact with the right wall Ω_R is

$$\Omega_R = \psi - \theta_{R0} + \frac{\pi}{2}. \qquad (1)$$

It is related to the surface energy of the crystal $\alpha(\theta)$, crystal-wall energy ε_s, and liquid-wall energy ε_l by the equation

$$\alpha(\theta_{R0}) \cos \Omega_R + \alpha'_\theta(\theta_{R0}) \sin \Omega_R = -\Delta\varepsilon, \qquad (2)$$

where $\Delta\varepsilon = \varepsilon_s - \varepsilon_l$

The angle of contact with the left wall is

$$\Omega_L = \psi + \theta_{L0} + \frac{\pi}{2}. \qquad (3)$$

The boundary condition near the left wall has the form

$$\alpha(\theta_{L0}) \cos \Omega_L - \alpha'_\theta(\theta_{L0}) \sin \Omega_L = -\Delta\varepsilon. \qquad (4)$$

The right and left walls are made of the same material (polished glass). Therefore, the same physical state should take place at both walls at the same values of ψ for the horizontal orientation of the basal plane in the crystal due to the presence of screw twofold axis C_2 in the symmetry group of the crystal. When C_2 rotates, angle θ_{L0} changes its sign and we will present experimental data for the general function $\theta_0(\psi) = \theta_{R0}(\psi) = -\theta_{L0}(\psi)$.

To control the possibilities of our optical technique, we used the results of digital processing of photographs taken from two test samples. Figure 2a shows shape $Z(x)$ of the meniscus of liquid ^{4}He filling the lower part of

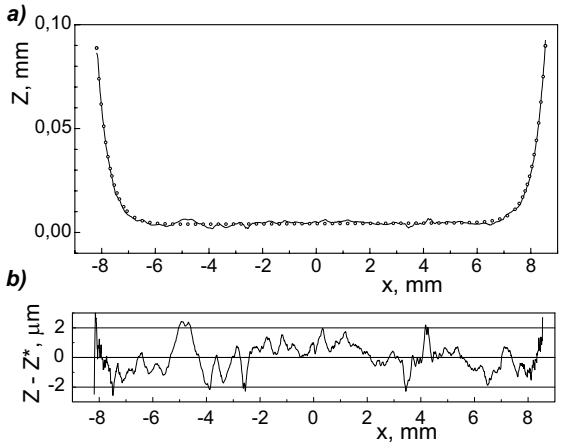

Fig. 2. *a)* (line) Shape $Z(x)$ of the meniscus of liquid ^{4}He and (circles) calculated profile. *b)* Deviation of the experimental from the calculated curve.

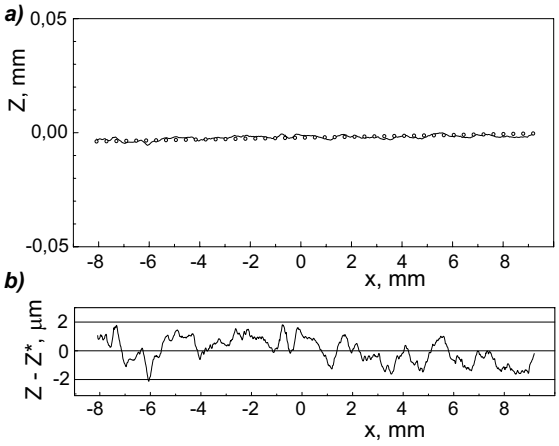

Fig. 3. *a)* Shape $Z(x)$ of a flat growing face of a ^{4}He crystal, and the dashed line shows the face direction. *b)* Deviation of the experimental curve from a straight line.

the chamber. Here, we also present the surface shape calculated in the low-angle approximation $\theta \ll 1$,

$$Z^*(x) = A + B\,\mathrm{ch}\,\frac{x}{\Lambda},\ \Lambda = \sqrt{\frac{\alpha_l}{\rho_l g}},$$

where $\alpha_l = 0{,}28\,\mathrm{erg/cm^2}$ — is the surface tension of liquid ^{4}He at $T = 2{,}3\,\mathrm{K}$ [3], $\rho_l = 0{,}145\,\mathrm{g/cm^2}$ — is its density, and g — is the gravitational acceleration. Figure 2b shows the dependence $\delta Z(x) = Z(x) - Z^*(x)$, which characterizes the deviation of an experimental curve from the calculated curve corresponding to the optimum choice of adjustable parameters A and B.

Similar data are presented in Fig. 3 for the crystal the (0001) plane of which is close to the horizontal. This photograph was taken at a temperature of 0.88 K, i.e., well below roughening temperature T_R of the basal plane. Under these conditions, the interface coincides with the growing face. In Fig. 3a, dependence $Z(x)$ is approximated by a straight line $Z^* = A + Bx$. The difference between the experimental results and the optimum straight line is shown in Fig. 3b. In both cases (Figs. 2b, 3b), the deviations from the real shape are random (about $\pm 2\,\mu$m) and are the main origin of errors in determining the surface shape. The image of the liquid helium meniscus can be used to detect the horizontal direction accurate to $\sim 2 \cdot 10^{-4}$ rad. Using photographs of a growing face, its direction in the xz plane was determined accurate to $\sim 2 \cdot 10^{-4}$ rad.

At the initial stage of experiments, we grew a small $\sim 1\,\mathrm{mm^3}$ crystal whose basal plane was close to the horizontal. This procedure was described in detail in [1, 2]. The crystal was then grown slowly to reach the level of the glass walls. The growth rate did not exceed $\sim 1\,\mu$m/s and was stabilized by controlled heating of the ballast volume outside the cryostat. The pressure in the ballast volume exceeded the equilibrium pressure by ~ 0.4 mbar.

After the chosen temperature was stabilized, we took photographs of the crystal profiles at various levels. The transitions to the next levels were performed by sequential surface melting or growing of the crystal. The difference between neighboring levels was 0.2–0.5 mm.

Once the next level was reached, the chamber with the crystal was disconnected from the ballast volume with a valve located outside the cryostat at room temperature[1)]. As a result, quasi-equilibrium conditions, which are accompanied by a very slow helium flow from the filling line to the chamber because of a low level of liquid helium in the cryostat bath at 4.2 K, were established. Under these conditions, the crystal grew slowly at a rate of $\sim 5 \cdot 10^{-3}\,\mu$m/s and had almost the same shape.

We now present the measurement results for two crystals. In the first sample, the basal plane was inclined at an angle of $2 \cdot 10^{-4}$ rad in the transverse direction (with respect to axis x) and at an angle of $1,2 \cdot 10^{-3}$ rad in the longitudinal direction (with respect to axis y). For the second sample, the transverse inclination was $8 \cdot 10^{-4}$ rad and the longitudinal inclination was $6 \cdot 10^{-4}$ rad. After measuring the longitudinal face inclination, the optical bench was inclined at the measured angle; as a result, the error in parallelism between the optical axis and the crystal face was corrected.

[1)] Unfortunately, the design of our device does not imply the existence of a "cold" valve.

The first sample was photographed during gradual surface melting, and the second sample was grown gradually. In both cases, photographs were taken in 20 and 40 min after the chamber was closed with the valve in order to control surface relaxation. For the first sample, we took two series of photographs corresponding to temperatures of 0.89 and 0.61 K; for the second sample, three series of photographs were taken at temperatures of 0.9, 0.72, and 0.53 K.

The results of processing two of the five series are shown in Fig. 4 (first sample, $T = 0{,}61$ K) and Fig. 5 (second sample, $T = 0{,}9$ K). The scale in the ordinate axis is higher than that of the abscissa scale by more than 60 times. All curves are located as close as possible to each other without conserving the vertical scale. The real vertical distance between the centers of the upper and lower profiles is about 5 mm.

The situation seems to be ambiguous from the standpoint of an equilibrium surface shape.

An equilibrium surface shape is known to correspond to the minimum of the surface and gravitational energy, and the surface rigidity plays a key role in this case. In our case, we are dealing with so-called longitudinal rigidity $\tilde{\alpha} = \alpha + \alpha''$. The surface rigidity was studied by various methods [4, 5, 6]. The result substantial for us consist in the following. In the temperature range $0.4\,\mathrm{K} < T < T_R$, the surface rigidity has a weak anisotropy for atomically rough surface regions at sufficiently low angles of inclination ($\theta \lesssim 0{,}1$ rad). The rigidity is temperature-independent ($\tilde{\alpha}_0 \approx 0{,}245\,\mathrm{erg/cm^2}$). A sharp decrease in $\tilde{\alpha}$ was only detected [7] at temperatures below 0,3 K and low angles $\theta < 0{,}04$ rad.

For all series of our experimental data, surface regions at not very low angles of inclination ($10^{-2} \lesssim \theta \lesssim 0{,}1$ rad) obey the equilibrium equation

$$\tilde{\alpha} Z''_{xx} = \Delta\rho Z, \tag{5}$$

where $\tilde{\alpha} = 0{,}245\,\mathrm{erg/cm^2}$, and $\Delta\rho$ is the difference between the densities of the solid and liquid phases.

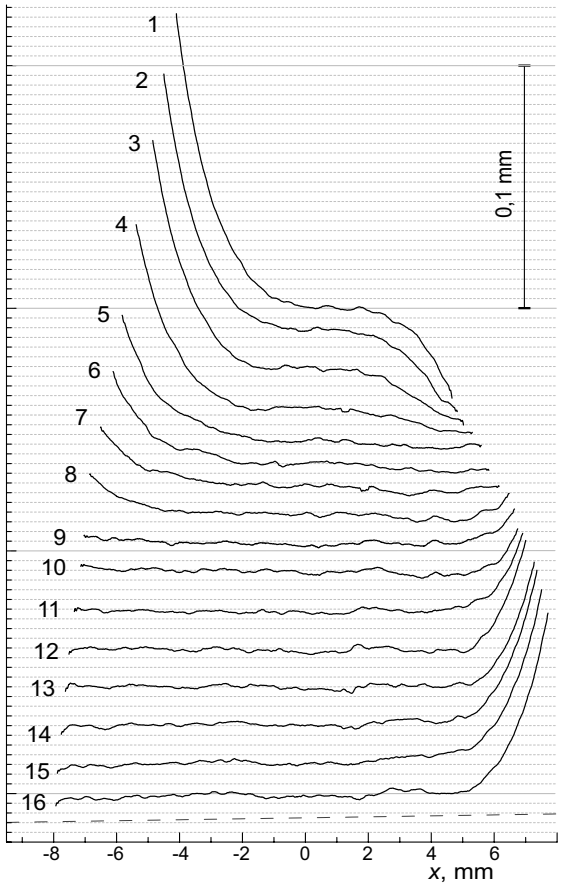

Fig. 4. Series of crystal menisci at $T = 0{,}61$ K. The face direction is indicated by the heavy dashed line. The photographs were taken during melting.

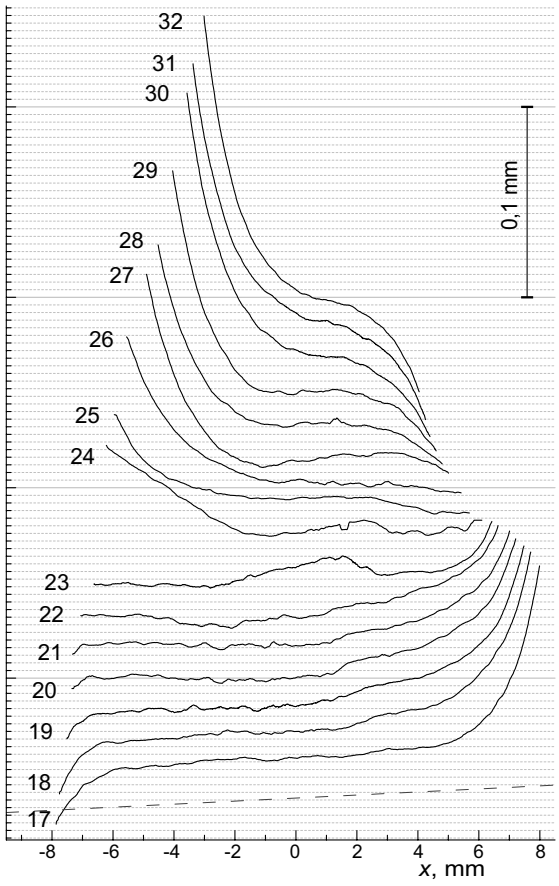

Fig. 5. Series of crystal menisci at $T = 0{,}9$ K. The face direction is indicated by the heavy dashed line. The photo- graphs were taken during growth.

Figure 6 shows the approximation[2)] of the profile 16 by the solution to Eq. (5), $Z = A\,\mathrm{sh}\,\frac{x-x_0}{\Lambda}$, where $\Lambda = (\tilde{\alpha}/\Delta\rho g)^{1/2}$. The dashed line shows the measured direction of the (0001) face inclined at $2 \cdot 10^{-4}$ rad to the horizontal. Similar results of processing profile 32 Fig. 5 are shown in Fig. 7. In this case, the left and right segments of the profile are approximated by the formula $Z_{\pm} = A\,\mathrm{sh}\,\frac{x-x_{\pm}}{\Lambda}$ at the same amplitude A and parameters $x_{\pm}$, differing by ≈ 1 mm.

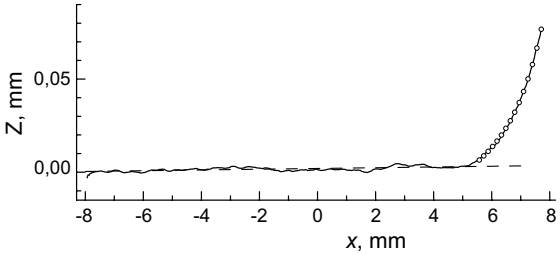

Fig. 6. Profile 16 (line) at $T = 0{,}61$ K and (circles) approximation of the meniscus.

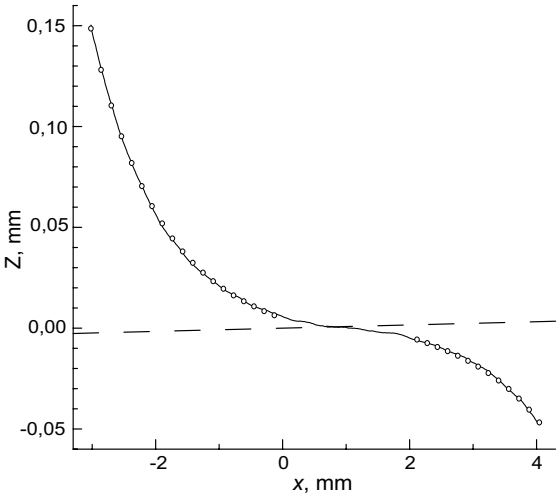

Fig. 7. (line) Profile 32 at $T = 0{,}9$ K and (circles) its approximation.

Thus, we can state that the surface is in equilibrium at not very low angles $10^{-2} \lesssim \theta \lesssim 10^{-1}$. The situation is radically different at angles $\theta \lesssim 10^{-2}$ rad: non-monotonic profiles often appear, which indicates the absence of equilibrium (see Figs. 5,4). The lengths of such regions along axis x change within several millimeters, and the irregular deviations from the vertical are $10 - -20\,\mu$m. Such phenomena are usually related to lattice defects, mainly dislocations, and we cannot exclude this explanation. We only recall that the crystals were grown with all precautions necessary in such cases.

However, the shapes of some surface fragments can hardly be explained by the presence of dislocations. For example, the center portion of profile 23 (Fig. 5) contains a linear (within the limits of experimental error) ~ 4 mm segment inclined at an angle of 0.003 rad to the (0001) face. The next frame (profile 24) contains a flat region reaching the left wall and inclined at an angle of 0.01 rad to the opposite side. The presence of such extended surface regions is thought to be hardly explained by the existence of defects in the crystal volume. Unfortunately, we have no certain considerations regarding the nature of these metastable states. It is difficult to draw any quantitative conclusions concerning the equilibrium meniscus shape (and the contact angle) and, hence, the angular dependence of the surface rigidity at low angles under these conditions.

The authors of [8] theoretically predicted a phenomenon caused by the jump of derivative α'_θ at $\theta = 0$. This phenomenon consists in the fact that the state where an atomically smooth face is in immediate contact with the wall takes place in the angular range $\psi_- < \psi < \psi_+$, determined by the relation

$$|\Delta\varepsilon - \alpha_0 \sin\psi| < \beta \cos\psi$$

where $\beta = \alpha'_\theta > 0$ at $\theta = +0$. In this case, a plateau should appear in the $\theta_0(\psi)$ dependence in a certain angular range. Figure 8 shows the results of processing our photographs for this dependence. The plateau is seen to exist. However, the $\theta_0(\psi)$ dependence differs substantially from the root behavior suggested in [8]. The contact angle approaches the plateau linearly at not very low angles $\theta_0 \sim 1^\circ$.

Recall that the meniscus profile was determined from an analysis of a diffraction pattern, as was described in our earlier works [1, 2]. However, it is difficult to perform this analysis near the crystal-liquid-wall contact line, i.e., in the region where the contact angle is to be determined. Here, the diffraction pattern is complicated because of the approaching of two relatively simple diffraction patterns from the wall and the crystal-liquid interface at a distance of ≈ 0.3 mm, which is comparable with $\Lambda \approx 1.2$ mm. The value of θ_0 at $\theta_0 > 0{,}01$ rad under these conditions was determined by the extrapolation of the derivative of the function approximating the meniscus $Z = A\,\mathrm{sh}\,\frac{x-x_0}{\Lambda}$ to the calculated point of contact with the wall. The region of low contact angles $\theta_0 \leq 0.01$ rad, where the root law is likely to be valid, requires an additional investigation.

[2)] Note that the meniscus shape can also be described [2] with a satisfactory accuracy by the function $Z = \pm(x - x_0)^3 b^{-2}$, where $b \sim 1$ mm, which corresponds to the standard theory of a vicinal surface as the echelon of steps that repel each other as $\propto x^{-2}$. However, this picture is in conflict with the results of measuring $\tilde{\alpha}$ from the spectrum of crystallization waves at not very low angles.

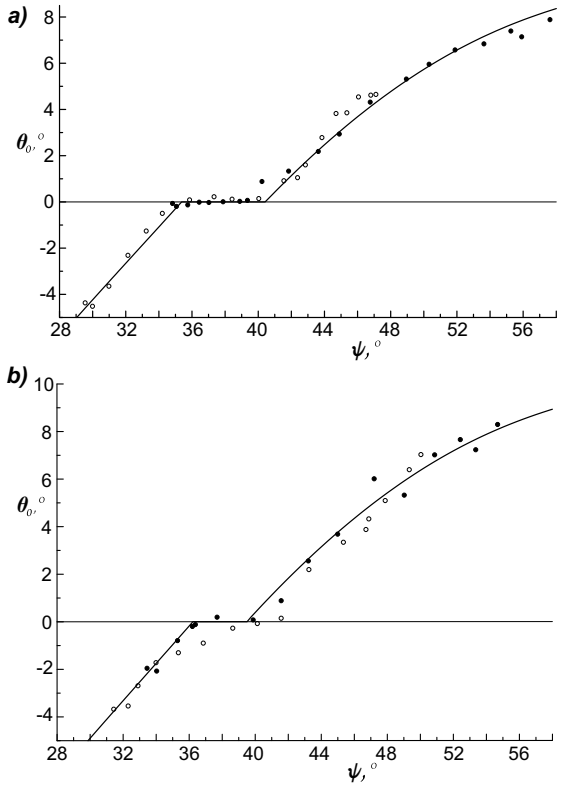

Fig. 8. Dependence $\theta_0(\psi)$ for two series of profiles obtained at *a)* $T = 0{,}61\,\mathrm{K}$ и *b)* $T = 0{,}9\,\mathrm{K}$. Open and solid symbols correspond to the right and left sides of a meniscus, respectively. (solid line) Calculation by Eqs. (2),(4),(6), and (7).

The observed behavior of the meniscus at angles $10^{-2} < \theta \lesssim 10^{-1}\,\mathrm{rad}$ can be explained under the following assumptions: function $\alpha(\theta)$ at these angles has the form

$$\alpha = \alpha_0 + \beta|\theta| + \alpha_0'' \frac{\theta^2}{2}, \qquad (6)$$

and solid helium-glass interface energy ε_s is a function of angle ψ. Moreover, we believe that, in the temperature range under study, only the step energy changes with temperature and the other parameters $\alpha_0 \approx 0{,}172\,\mathrm{erg/cm^2}$ [9], $\alpha_0'' = \tilde{\alpha}_0 - \alpha_0 \approx 0{,}073\,\mathrm{erg/cm^2}$, and function $\Delta\varepsilon(\psi)$ almost reached their values characteristic of zero temperature.

Figure 9 shows the $\Delta\varepsilon(\psi)$ function calculated by Eqs. (2) and (4) using the experimental data for the two series of measurements. Parameters β for each series were chosen so that the imaginary extensions of the $\Delta\varepsilon(\psi)$ functions calculated at $\psi < \psi_-$ and $\psi > \psi_+$, are matched in the plateau region. The results for the $\Delta\varepsilon(\psi)$ functions thus obtained coincide for both series within the limits of experimental error. We take into account the symmetry of the helium crystal, neglect the azimuthal anisotropy, assume that $\Delta\varepsilon(\psi)$ is an analytical function of angles, and parametrize it as (in $\mathrm{erg/cm^2}$)

$$\Delta\varepsilon(\psi) = 0{,}128 - 0{,}013\cos 2\psi + 0{,}022\cos 4\psi, \qquad (7)$$

The calculated $\theta_0(\psi)$ dependence with allowance for the anisotropy of $\Delta\varepsilon(\psi)$ (see Eq. (7)) are shown as the solid lines in Fig. 8.

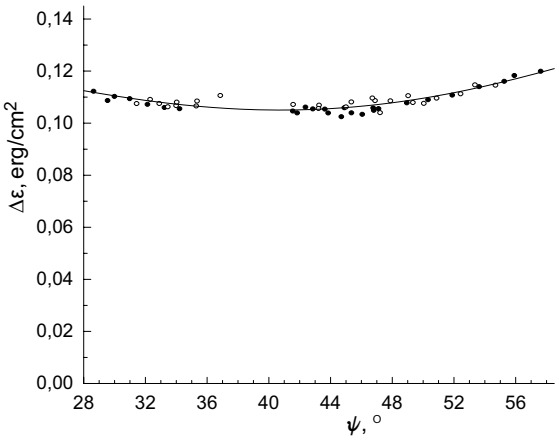

Fig. 9. Dependence $\Delta\varepsilon(\psi)$ plotted from the data of the two series of measurements at $T = 0{,}9\,\mathrm{K}$ (open symbols) and (solid symbols) $T = 0{,}61\,\mathrm{K}$ (solid line) Calculation by Eq. (7).

Using this scheme and Eq. (7), we then determined the values of β for the other series[3)].

The obtained temperature dependence of β is shown in Fig. 9 (solid circles). Here, we also present the results from [7] (open circles), which were obtained in the temperature range $50 \div 250\,\mathrm{K}$ by an analysis of a spectrum of crystallization waves, and from [4] (open triangles), which were obtained by an analysis of the (0001) face growth kinetics at temperatures close to the roughening temperature, and the value of β obtained in [1] (cross) at a temperature of $0.72\,\mathrm{K}$.

Thus, our data on β characterizing the surface energy at angles $0,01 < \theta \lesssim 0,1\,\mathrm{rad}$ agree with the data in [7] obtained at $\theta \lesssim 0,01\,\mathrm{rad}$. However, the authors of [7] detected a sharp decrease in $\tilde{\alpha}$ at temperatures lower than $0.25\,\mathrm{K}$ and angles $\theta \lesssim 0,01\,\mathrm{rad}$, which agrees with the theoretical concepts of vicinal surfaces, and we detected non-analytical contribution $\beta|\theta|$ to the surface energy in the angular range $0,01 < \theta \lesssim 0,1\,\mathrm{rad}$, which cannot be explained theoretically at finite and weakly temperature-dependent $\tilde{\alpha}$.

[3)] Note that the neglect of anisotropy $\varepsilon_s(\psi)$ leads to an increase in the estimate of β by about 30%.

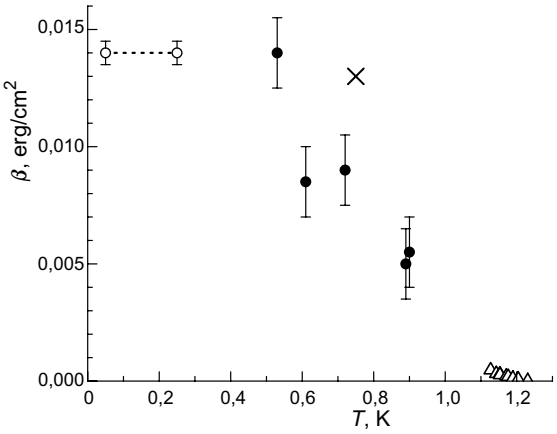

Fig. 10. Dependence $\beta(T)$.

We thank A.F. Andreev, A.Ya. Parshin, and E.R. Podolyak for fruitful discussions. This work was performed in terms of the fundamental research program Quantum Mesoscopic and Disordered Structures of the Presidium of the Russian Academy of Sciences.

1. K.O. Keshishev, V.N. Sorokin, and D.B. Shemyatikhin, JETP Lett. **85**(3), 179 (2007)
2. K.O. Keshishev, D.B. Shemyatikhin, JLTP **150**, 282 (2008)
3. J.F. Allen, A.D. Misener, Math. Proc. of the Cambridge Phil. Soc. **34**, 299 (1938)
4. P.E. Wolf, F. Gallet, S. Balibar, P. Nozierès, J. Physique (France) **46**, 1987 (1985)
5. A.V. Babkin, D.B. Kopeliovich, and A.Ya. Parshin, Sov. Phys. JETP **62**(6), 1322 (1985)
6. O.A. Andreeva, K.O. Keshishev, and S.Yu. Osip'yan, JETP Lett. **49**(12), 759 (1989)
7. E. Rolley, C. Guthmann, E. Chevalier, S. Balibar, JLTP **99**, 851 (1995)
8. V.I. Marchenko and A.Ya. Parshin, JETP Lett. **83**(9), 416 (2006).
9. O.A. Andreeva and K.O. Keshishev, Phys. Scr., **39**, 325 (1991).

Translated by K. Shakhlevich

JETP **116**(4), 587 (2013)